Journal of Catalysis 363 (2018) 144–153

Contents lists available at ScienceDirect

Journal of Catalysis

journal homepage: www.elsevier.com/locate/jcat

Low-temperature selective oxidation of methanol over Pt-Bi bimetallic catalysts

Yang Xiao, Yuan Wang, Arvind Varma *

Davidson School of Chemical Engineering, Purdue University, West Lafayette, IN 47907-2100, United States

ARTICLE INFO

Article history:
Received 6 January 2018
Revised 11 March 2018
Accepted 13 April 2018

Keywords:
Low-temperature selective oxidation
Methanol to formaldehyde
Bimetallic catalysts
Correlation of catalyst property and performance
Oxidation of alcohols to aldehydes

ABSTRACT

Formaldehyde is industrially produced by methanol selective oxidation over supported Ag or Mo-Fe catalysts in the temperature range 250–600 °C. The development of relatively low temperature processes for formaldehyde production is of importance to decrease energy costs and capital investment resulting from the high temperature operation. In the present work, various Pt-Bi bimetallic catalysts were designed, prepared, characterized and tested for low temperature (70–120 °C) methanol selective oxidation to formaldehyde. The highest selectivity toward formaldehyde (98.1%) at methanol conversion (8.1%) was achieved over the 1% Pt–0.5% Bi/AC (activated carbon) catalyst. Utilizing various characterization techniques (BET, EDX, H_2-O_2 titration, H_2-TPR, ICP-AES, TEM, TPO, XPS and XRD) along with catalytic activity tests, the properties and performance of Pt-Bi bimetallic catalysts were correlated. The reducibility of Pt-Bi catalysts shows a linear relationship with formaldehyde selectivity, while methanol turnover frequency (TOF) values are essentially constant. Considering methanol as a simple molecule probe, the present work offers potential opportunities for selective oxidation of other alcohols at relatively low temperatures.

© 2018 Published by Elsevier Inc.

1. Introduction

Selective partial oxidation of alcohols (e.g. methanol, ethanol, glycerol, etc.) over heterogeneous catalysts plays an important role in the production of bulk and fine chemicals, as well as in the conversion of biomass-derived compounds to renewable fuels and high value-added products [1,2]. The correlation between catalyst properties and performance (conversion and selectivity towards a target product) benefits the development of efficient catalytic processes [3,4].

Methanol, the simplest alcohol, is used as a solvent, fuel for specialized vehicles or feedstock for manufacture of other value-added chemicals, including formaldehyde and olefins [5,6]. Methanol is considered as the simplest molecule probe candidate, owing to its representative structure, containing C-H, C-O and O-H bonds [7,8]. About 40% of industrial methanol is converted to formaldehyde, and subsequently into diverse products such as plastics, plywood, paints and fibers, while the remaining methanol is consumed in the manufacture of textiles, paper, fertilizers, miscellaneous resinous products [9]. Formaldehyde is produced commercially by catalytic selective oxidation of methanol, where the most common processes utilize supported silver (Ag) or molybdenum-iron (Mo-Fe) catalysts [9,10]. The silver process operates at atmospheric pressure and temperature in the range 560–600 °C. Under these conditions, methanol conversion is typically 65–75%, while formaldehyde selectivity is about 90%. In the Mo-Fe process, an excess of air is used to ensure nearly 100% conversion and avoid the explosive limits of methanol (6.7–36.5 vol.% in air). The reaction temperature is lower than that for the silver process, but yet in the range 250–400 °C. The formaldehyde yield is improved to 95%, with conversion as high as 98–99%. Other catalyst candidates for methanol selective oxidation to formaldehyde have also been reported in the literature, including VO_x (~400 °C) [11–13], Cr-Mo (~300 °C) [14], Fe-Cr-Mo (~300–360 °C) [15,16], Mo-V-Cr-Bi-Si (~425 °C) [17], MoO_3 (~300–350 °C) [18] and Bi_2O_3-MoO_3 (280 °C) [19]. The use of a membrane-distributed feed reactor to enhance yield has also been investigated [20,21]. In all these cases, however, relatively high temperature (250–600 °C) is always used, leading to high energy and operating costs as well as large capital investment.

Using noble metals such as Pt or Pd, low-temperature ($\lesssim$ 120 °C) oxidation of methanol has been investigated previously. Owing to the superior activity over noble metals, however, formaldehyde production is limited using these catalysts because over-oxidized products (e.g. formic acid and CO_2) are typically generated [22–24]. Using controlled Pd nano-particles with specific metal particle size as catalyst, the formaldehyde selectivity was

* Corresponding author.
E-mail address: avarma@purdue.edu (A. Varma).

https://doi.org/10.1016/j.jcat.2018.04.016
0021-9517/© 2018 Published by Elsevier Inc.

only 20–30% [25]. The use of Pt-based catalysts for formaldehyde production from methanol oxidation have also been reported. These, however, result in either low methanol conversion (<2.5%) [26,27], or low selectivity towards target formaldehyde product [28,29]. Recently, rather than over-oxidized products and formaldehyde, methyl formate was selectively (with selectivity > 95%) synthesized by methanol coupling over Au catalysts [30]. Similar high selectivity values towards methyl formate were also achieved over Pd-based catalysts [31].

In general, reducible oxides (CeO_2, TiO_2, V_2O_5, Bi_2O_3, etc.) can achieve high selectivity for certain non-over-oxidized products [32]. Among these, bismuth oxides show flexible oxidation states, including +1 to +5, and typically +3. This suggests that Bi is a potentially good catalytic promoter for selective oxidation [33]. When reducible oxides are used as promoters in addition to noble metals, noble metal/reducible oxide interfaces are formed, which are able to tune selectivity towards target products by providing surface oxygen vacancy [34]. In our prior studies, some applications of bimetallic Pt-Bi catalysts were reported, e.g. glycerol conversion to 1,3-dihydroxyacetone (DHA) [35,36], guaiacol deoxygenation by the use of methane as reductant [37,38], and highly selective nonoxidative coupling of methane (NOCM) to C_2 species [39]. Using density functional theory (DFT) [40], we concluded that the BiO_x species is formed *in situ* at the interface of the originally reduced Pt-Bi bimetallic catalyst. A cooperative effect between Pt as the primary component and BiO_x as the promoter was further identified for DHA formation from glycerol oxidation. Thus the Pt-BiO_x interface favors O-H, rather than C-H, bond breaking. To our knowledge, there is currently no available method which converts methanol to formaldehyde with high selectivity (e.g. >90%) at temperature $\lesssim$ 120 °C.

In the present work, as a chemical probe molecule, methanol is converted to formaldehyde with high selectivity at relatively low temperatures. Based on performance tests in a fixed-bed reactor and catalyst characterization results, methanol conversion and selectivity toward formaldehyde are correlated with the properties of Pt-Bi catalysts. The catalytic mechanism and reaction pathway are proposed and discussed. The insight into selective oxidation of methanol over Pt-Bi bimetallic catalysts provided in this work may lead to applications of similar bimetallic catalysts in selective oxidation of other alcohols.

2. Experimental

2.1. Materials and catalyst preparation

The chloroplatinic acid hexahydrate (99.9% metal basis) and bismuth (III) chloride (99.999%), both from Sigma Aldrich, were used as precursors for Pt and Bi, respectively. The commercial bismuth (III) oxide was from Alfa Aesar. The activated carbon (AC) of 80–120 mesh, from Norit Americas Inc., was used as the catalyst support. The Pt-Bi catalysts were prepared by the following procedure as described in our prior works [35,37]. Pt and Bi were loaded sequentially, in that order, by the wet impregnation method. The Pt and Bi precursors were dissolved in diluted HCl solution and then added dropwise to the well-stirred AC slurry, with continued stirring for 8 h at room temperature (20 °C). The slurry was then rinsed two times and dried in air at 100 °C before use. Since chloride ions dissolve in aqueous solutions, either limited or zero content of chloride ions is expected in Pt-Bi catalysts. Methanol (99%) and all other calibration compounds, including formaldehyde (37 wt% in water, with 7–8% methanol as stabilizer), methyl formate (97%), dimethoxymethane (98%) and formic acid (97%), were from Alfa Aesar. Ultra high purity grade gases (99.98% O_2, 99.999% Ar, 99.999% N_2, 99.98% He, 99.99% CO_2 and 99.999% H_2) were purchased from Indiana Oxygen. The 0.5 wt% Pt/Al_2O_3 (metal dispersion = 31 ± 0.5%) standard, from Micromeritics, was used for H_2-O_2 titration calibration.

In this work, the Pt and Bi loadings were always on the AC support with a weight (wt) basis. For this reason, in later sections the weight basis and AC support are not noted explicitly when describing the catalysts. Thus, e.g., 1% Pt–1% Bi sample refers to 1 wt.% Pt and 1 wt.% Bi loaded on the AC support.

2.2. Catalyst characterization

Various Pt-Bi catalysts used in the present work were characterized by BET (Brunauer-Emmett-Teller), H_2-TPR (Temperature-programmed reduction), ICP-AES (Inductively coupled plasma – atomic emission spectroscopy), TEM (Transmission electron microscopy), TEM-EDX (Energy-dispersive X-ray), TPO (Temperature-programmed oxidation), XPS (X-ray photoelectron spectroscopy) and powder XRD (X-ray diffraction) techniques.

By N_2 adsorption and desorption at 77 K via a Micromeritics ASAP 2000 apparatus, BET measurements were conducted, giving physisorption properties of catalysts, including surface area, pore size and pore volume. Prior to measurements, degassing was carried out at 300 °C for 8 h. Using 0.5 wt% Pt/Al_2O_3 as calibration standard, Pt dispersion was obtained by the H_2-O_2 titration approach [41]. Note that at room temperature, Bi does not adsorb H_2 molecules [42] and bismuth oxide does not react with H_2 [43]. The TEM scans were operated at 200 kV with LaB_6 source (FEI-Tecnai). The TEM samples were prepared by suspending fine catalyst particles in ethanol, followed by dispersing them on 200 copper mesh grids with lacey carbon film coating, and then drying in air at room temperature. The TEM-EDX scans were carried out using a FEI Talos F200X scanning transmission electron microscope. EDX was done using X-FEG high-brightness electron source. The XPS measurements were performed on a Kratos spectrometer equipped with a multichannel hemispherical electron energy analyzer. A monochromatic Al Kα line ($h\nu$ = 1486.7 eV, power = 250 W) was used under ultra-high vacuum conditions. The powder XRD was carried out on an Rigaku SmartLab X-ray diffractometer with a CuKα radiation source. Elemental analysis of catalysts was carried out by the ICP-AES method using a SPECTRO Instrument.

For H_2-TPR tests, 5 vol% H_2 and 5 vol% O_2 in N_2, prepared *in situ* by adjusting their flow rates via mass flow controllers, were used as reducing and oxidizing gases, respectively. The standard H_2-TPR operations included the following steps:

(i) Drying the sample at 200 °C in 5 vol% O_2 for 1 h;
(ii) Reducing the sample at 450 °C in 5 vol% H_2 for 2 h;
(iii) Re-oxidizing the sample at 120 °C in 5 vol% O_2 for 1 h [44];
(iv) H_2-TPR measurements by feeding 5 vol% H_2 in the range from room temperature to 700 °C.

The heating rate was 5 °C/min and the standard catalyst packed weight was 0.50 g. The total gas flow rate was 100 mL/min. The H_2 consumption was measured by a binary gas analyzer equipped with a thermal conductivity detector (TCD). In the TPO process, 5% O_2 in N_2 gas mixture was used as the oxidizing gas. The used catalysts were packed in the reactor for TPO measurements without any pretreatment. The heating rate was 5 °C/min as well.

2.3. Catalytic performance tests and product analysis

The catalytic performance tests were conducted in a fixed-bed reactor. Prior to reaction, the packed catalyst was activated at 450 °C for 4 h under a gas mixture flow (H_2:N_2 = 1:2). The reactor was then purged by 50 mL/min N_2 for 15 min. The standard

operating conditions were: 70 °C, 1 atm, 0.02 g catalyst, methanol feed rate 0.6 mL/h (liquid, at room temperature), preheated at 70 °C before entering the reactor, total gas flow rate 100 mL/min (corresponding to 6% CH_3OH, 1.5% O_2 and 92.5% N_2). The feed rates corresponded to a molar ratio of 4:1 between CH_3OH and O_2, as 50% of the O_2 stochoimetric value described by Eq. (1). The use of less O_2 for standard operating conditions was to suppress the generation of over-oxidized products (formic acid, CO_2, etc.).

$$2CH_3OH + O_2 \rightarrow 2HCHO + 2H_2O, \quad (1)$$

All data reported in the present work for catalytic performance comparison was taken at 0.5 h TOS. Blank tests of AC support with no Pt or Bi loading were carried out under standard operating conditions, with methanol conversion always less than 0.5%. All experiments had carbon mass balances of 94 ± 2%. Possible factors affecting mass balance include liquid hold-up in various locations in the system. A GC (Agilent GC6890) with flame ionization detector (FID), equipped with a DB-1701 column (30 m × 0.25 mm) was used for quantitative analysis of liquid products. The gaseous effluent was analyzed using a Micro GC (Agilent 3000A) equipped with two columns (Column A, MolSieve 5 A, 10 m × 0.32 mm; Column B: Plot U, 8 m × 0.32 mm) and two TCDs. All experiments were repeated at least twice and good repeatability generally within less than 2% deviation was achieved for all quantitative analysis.

Table 1
BET characterization results of various catalytic materials.

Catalyst	BET surface area, m^2/g	Pore size, nm	Pore volume, cm^3/g
1%Pt	583	3.4	1.2
1% Pt–0.2% Bi	539	3.8	1.5
1% Pt–0.33% Bi	567	3.2	1.1
1% Pt–0.5% Bi	521	3.4	1.1
1% Pt–1% Bi	508	2.9	0.9
1% Pt–2% Bi	535	3.0	1.0
2% Bi	511	2.6	0.7
Bulk Bi_2O_3	6	12.2	0.22

Table 2
ICP-AES element analysis of various catalytic materials.

Catalyst	Pt % (fresh)	Bi % (fresh)	Pt % (used)	Bi % (used)
1% Pt	0.97	–	0.93	–
1% Pt–0.2% Bi	0.94	0.21	0.92	0.19
1% Pt–0.33% Bi	0.97	0.35	0.94	0.33
1% Pt–0.5% Bi	0.95	0.48	0.93	0.46
1% Pt–1% Bi	0.94	1.08	0.92	1.06
1% Pt–2% Bi	0.98	2.06	0.95	2.03
2% Bi	–	2.03	–	1.98

3. Results and discussion

3.1. Catalyst characterization

As shown in Table 1, all catalysts supported on AC exhibited high surface areas in the range 500–600 m^2/g, pore size in the

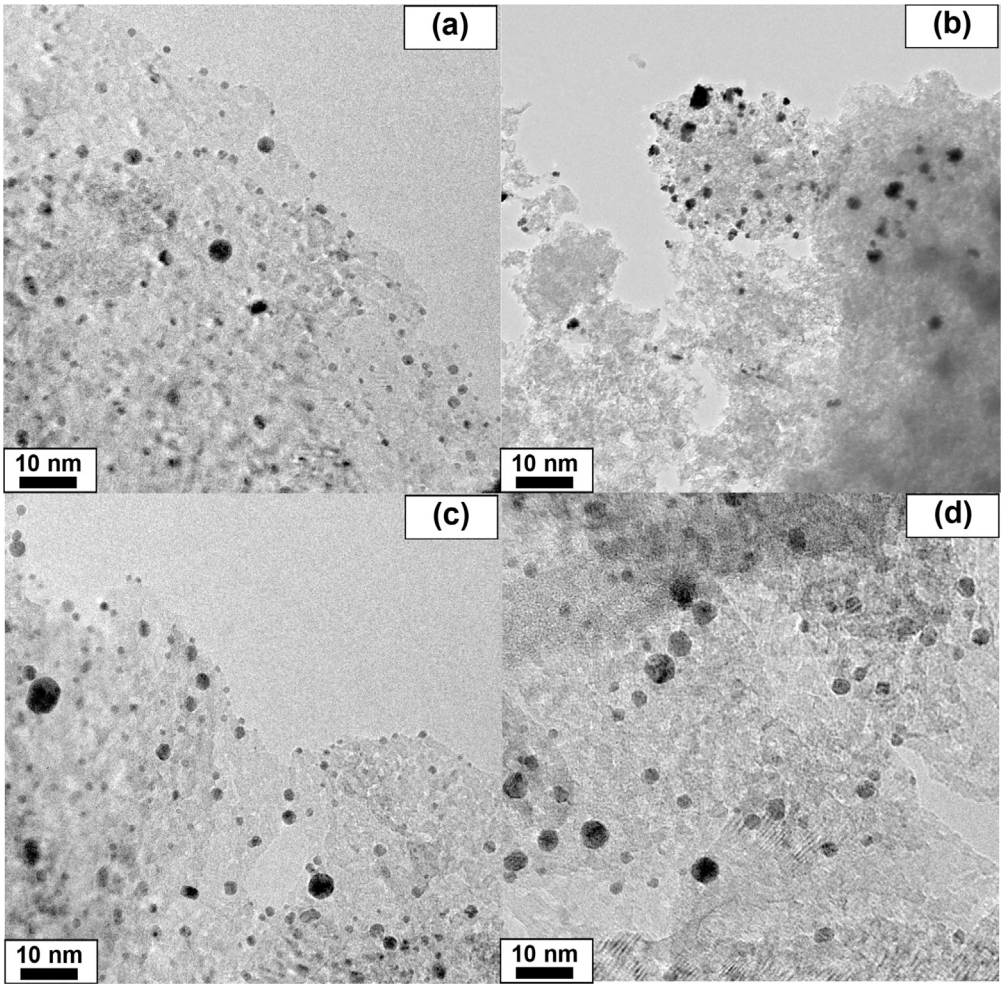


Fig. 1. TEM scans for (a) 1% Pt, (b) 1% Pt-0.2% Bi, (c) 1% Pt-0.33% Bi and (d) 1% Pt-2% Bi.

range 2.6–3.8 nm and pore volume in the range 0.7–1.5 cm^3/g. For bulk Bi_2O_3, all these values were very different. The data for both AC-based materials and bulk Bi_2O_3 was consistent with our prior works and literature reports [35,45,46]. The elemental analysis results of various Pt-Bi catalysts are listed in Table 2. For fresh catalysts, both Pt and Bi compositions were close to the designed metal loading values, while for used catalysts, 2–4 wt% loss was found for both metals. This unavoidable metal leaching was typically reported in the literature [47,48]. In the present study, the XRD patterns of various bimetallic Pt-Bi catalysts showed no significant peaks in the range of 5–90°. As reported in the literature [35,49–51], small particle size (<3 nm) and low metal loading (<5 wt%) and large background from amorphous catalyst supports usually make detection of such nano-particles very difficult. The TEM scans of four representative Pt-Bi bimetallic catalysts are shown in Fig. 1 and indicate that metals (dark dots) were successfully loaded on AC supports. Table 3 shows that Pt dispersion values were in the range 18.1–29.7%, while metal particle size values calculated by TEM scans and H_2-O_2 titration [52] were consistent.

The H_2-TPR profiles of various catalytic materials used in the present work are shown in Fig. 2. Based on quantitative Pt^{2+} and Bi^{3+} reduction [53,54], the H_2 consumption was calculated by integrating the curves in Fig. 2 and is listed in Table 4. The untreated 1% Pt (without H_2 reduction treatment after calcining the as-prepared material) started to reduce at ~100 °C, lasting until 500 °C, and a reduction peak appeared at about 200 °C. In contrast, the re-oxidized (after reduction) 1% Pt was reduced between room

Table 3
TEM, H_2-O_2 titration results and Turnover Frequency (TOF) values under standard operating conditions for various catalytic materials.

Catalyst	Particle size, nm		Pt dispersion, %	TOF, s^{-1}
	TEM	H_2-O_2 titration		
1% Pt	2.7	3.2	29.7	1.41
1% Pt–0.2% Bi	3.7	3.3	27.4	1.37
1% Pt–0.33% Bi	3.5	3.6	25.2	1.34
1% Pt–0.5% Bi	3.2	3.6	24.9	1.31
1% Pt–1% Bi	3.8	3.7	22.3	1.30
1% Pt–2% Bi	4.3	4.0	18.1	1.31
2% Bi	3.9	–	–	–

Table 4
H_2 temperature-programmed reduction (H_2-TPR) results of various treated catalytic materials.

Catalyst	H_2 consumption, $\mu L/g_{cat}$			Reducibility, %
	Experiment	Theory for Pt^{2+}-Bi^{3+}	Theory for Pt^{2+}-Bi^{+}	
1% Pt	1098	1149	1149	95.6
1% Pt–0.2% Bi	1410	1471	1256	95.6
1% Pt–0.33% Bi	1499	1680	1326	89.2
1% Pt–0.5% Bi	1687	1954	1471	86.3
1% Pt–1% Bi	2502	2758	1685	90.7
1% Pt–2% Bi	4215	4367	2221	96.5
2% Bi	3084	3218	1072	95.8
Used 1% Pt–0.5% Bi	1723	1954	1471	88.2

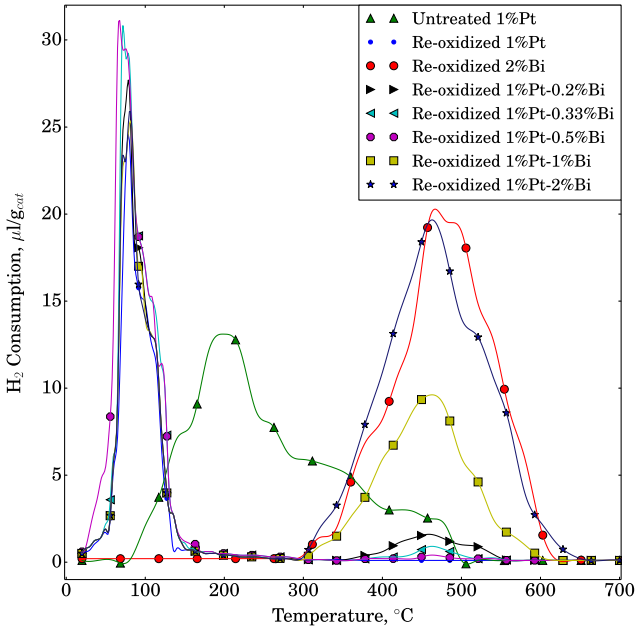


Fig. 2. H_2 temperature-programmed reduction (H_2-TPR) of various catalytic materials.

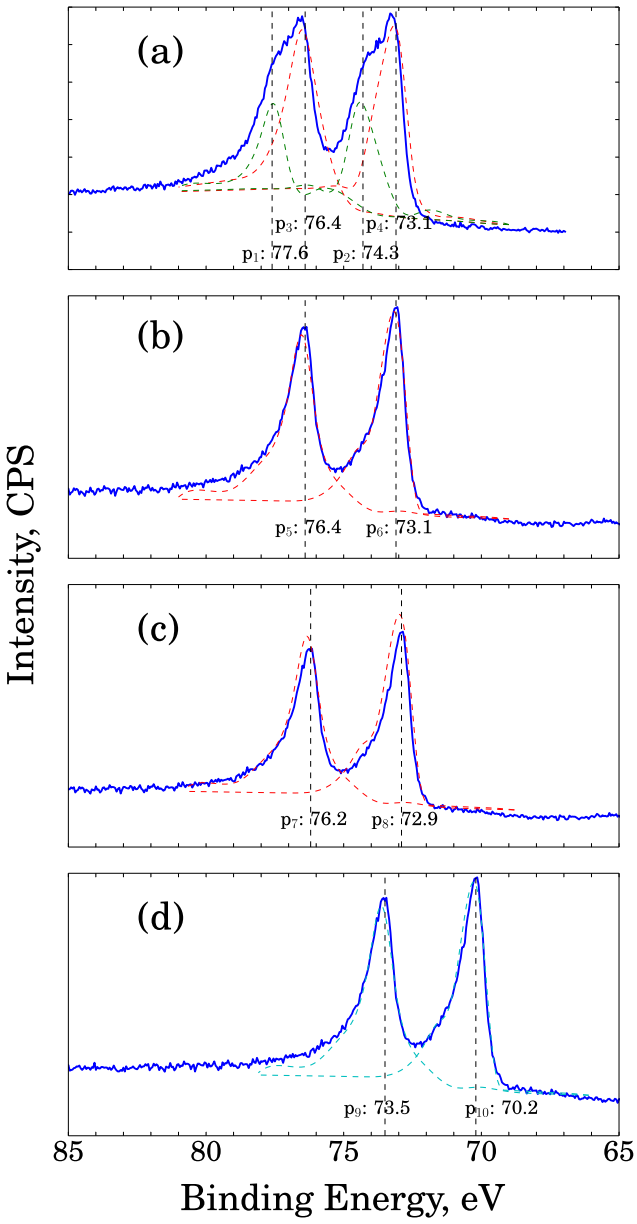


Fig. 3. XPS spectra of Pt 4f for (a) untreated 1% Pt, (b) re-oxidized 1% Pt, (c) re-oxidized 1% Pt-0.5% Bi and (d) reduced 1% Pt-0.5% Bi.

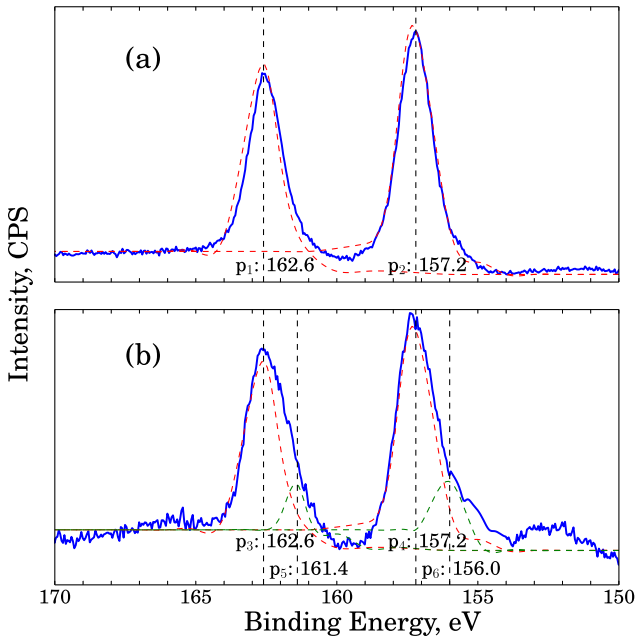


Fig. 4. XPS spectra of Bi 4f for (a) re-oxidized 1% Pt-0.5% Bi and (b) reduced 1% Pt-0.5% Bi.

temperature to 150 °C, with a reduction peak at ca. 100 °C. The total H_2 consumption of the re-oxidized [i.e. after step (iii) of the H_2-TPR procedure] 1% Pt was 1098 μL/g_{cat} (see Table 4), which was close to the theoretical H_2 consumption for Pt^{2+} reduction (1149 μL/g_{cat}). The untreated 1% Pt H_2-TPR curve, however, resulted in a larger H_2 consumption, likely owing to higher oxidized status of Pt (e.g. Pt^{4+}) and/or adsorbed organic species over the catalyst surface. The shift of reduction peak location to lower temperature suggests the ease of reducibility for re-oxidized 1% Pt catalyst, as compared to the untreated one. This also clarifies the need for catalyst activation by H_2 treatment prior to performance tests, as described in the Experimental section.

In Fig. 2, 2% Bi catalyst showed no reduction peak before 300 °C, while reduction occurred between ca. 300–600 °C. The reduction peak was at 450–500 °C, consistent with Bi_2O_3 reduction as reported in the literature [55]. In Table 4, the H_2 consumption data for 2% Bi was 3084 μL/g_{cat}, close to Bi^{3+} reduction (3218 μL/g_{cat}). For re-oxidized 1% Pt–0.2% Bi, 1% Pt–0.33% Bi and 1% Pt–0.5% Bi, two reduction peaks were observed, with the first at about 80–100 °C, and the second at about 450–500 °C, corresponding to Pt^{2+} and Bi^{3+}, respectively. As discussed in the literature [44], at about 100 °C, Pt species is oxidized to PtO (+2), while 300 °C oxidizes Pt species to PtO_2 (+4). Interestingly, with increase of Bi content (maintaining the same 1% Pt content), the Bi^{3+} reduction peak

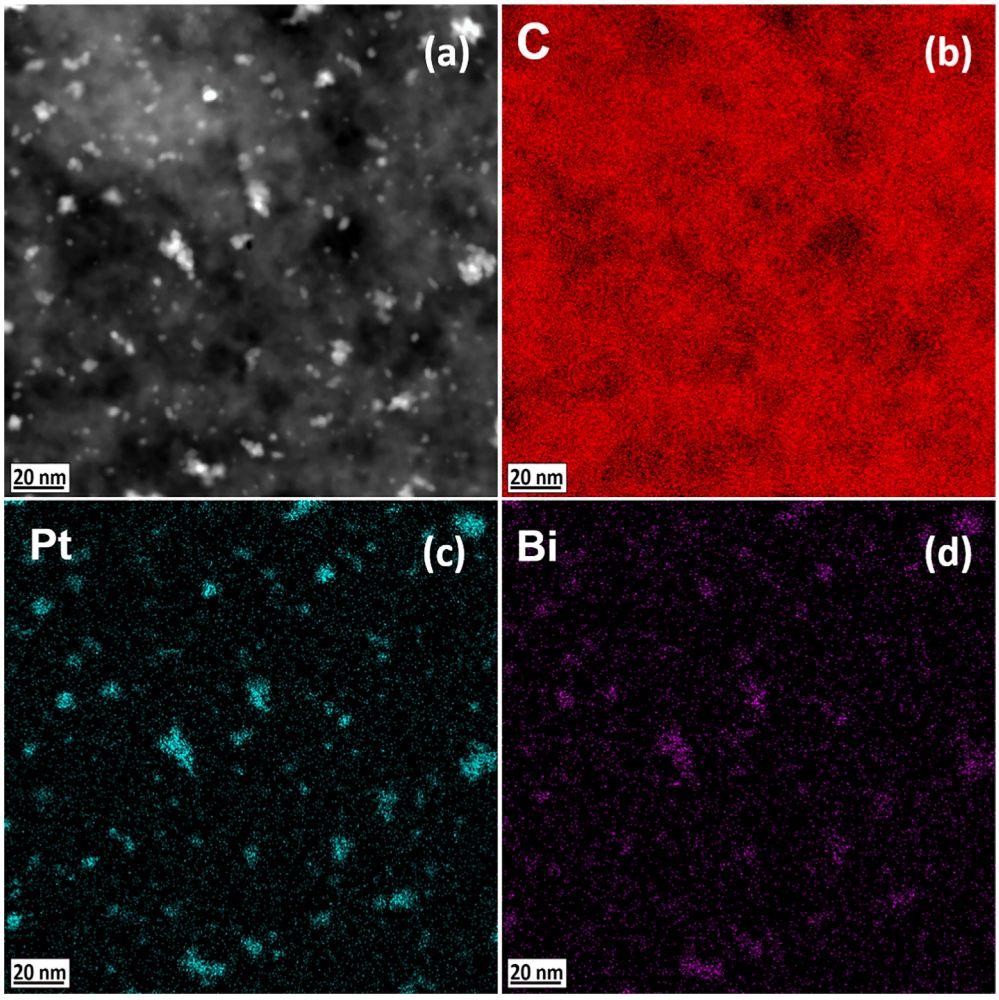


Fig. 5. (a) TEM scan of 1% Pt-0.5% Bi, (b–d) TEM-EDX mapping of 1% Pt-0.5% Bi for C, Pt and Bi.

areas decreased in these three catalysts, while Pt^{2+} reduction peak areas increased slightly. As reported in our prior work, Bi^{+} was proposed for the active site at Pt-Bi interface for selective oxidation of glycerol [40], indicating interaction between the two metals. Hence theoretical H_2 consumption values for Pt^{2+} and Bi^{+} reduction were also calculated in Table 4. It appears for all catalysts, the experimental H_2 consumption was larger than prediction of Pt^{2+} and Bi^{+} reduction. For 1% Pt–0.33% Bi and 1% Pt–0.5% Bi, however, the values were closer to Pt^{2+} and Bi^{+} than to Pt^{2+} and Bi^{3+}. The total experimental H_2 consumptions for these two catalysts were smaller than theoretical values for Pt^{2+}-Bi^{3+} reduction. These features indicate strong interaction between Pt and Bi in the presence of oxygen [56]. For the other two catalysts (1% Pt–1% Bi and 1% Pt–2% Bi), Bi^{3+} reduction showed large peaks, while Pt^{2+} reduction exhibited essentially the same magnitude peaks as the pure 1% Pt case. The total H_2 consumptions of these two relatively high Bi content catalysts were close to theoretical values for Pt^{2+}-Bi^{3+} reduction, suggesting that in these cases, Pt and Bi likely did not interact closely.

To further elaborate H_2 consumption of various Pt-Bi catalysts quantitatively, an index of reducibility is defined by Eq. (2).

$$Reducibility = \frac{Experimental\ H_2\ consumption}{Theoretical\ H_2\ consumption\ for\ Pt^{2+}\ and\ Bi^{3+}} \quad (2)$$

Reducibility values, suggesting interaction between Pt and Bi metals, are shown in Table 4. As described in later sections, reducibility is correlated with formaldehyde selectivity from methanol conversion.

The XPS spectra of Pt (4f) and Bi (4f) for various catalytic materials are shown in Figs. 3 and 4, respectively. As demonstrated in Fig. 3(a), the untreated 1% Pt suggests two oxidized states - Pt^{4+} (p_1: 77.6 eV and p_2: 74.3 eV) and Pt^{2+} (p_3: 76.4 eV and p_4: 73.1 eV) [57]. For re-oxidized 1% Pt, however, only Pt^{2+} (p_5: 76.4 eV and p_6: 73.1 eV) state is identified (Fig. 3(b)). Similarly, for re-oxidized 1% Pt-0.5% Bi, Pt^{2+} (p_7: 76.2 eV and p_8: 72.9 eV) is the only oxidized state (Fig. 3(c)). As compared to the pure Pt catalyst, the slightly different Pt^{2+} binding energy values (by 0.2 eV) in the Pt-Bi bimetallic catalyst likely owe to interaction between Pt and Bi species, because such shifts suggest partial electron transfer from Bi to Pt. As demonstrated in Fig. 3(d), Pt^{0} (p_9: 73.5 eV and p_{10}: 70.2 eV) is the primary Pt species in reduced 1% Pt–0.5% Bi, indicating full reduction of Pt. The Pt oxidized states for these catalysts are consistent with H_2-TPR measurements (Table 4 and Fig. 2). In Fig. 4(a), bismuth exhibits Bi^{3+} (p_1: 162.6 eV and p_2: 157.2 eV) in the bimetallic Pt-Bi catalyst, as reported in the literature [58] and our H_2-TPR measurements. For reduced 1% Pt–0.5% Bi, the majority Bi species is Bi^{3+} (p_3: 162.6 eV and p_4: 157.2 eV), while Bi^{0} (p_5: 161.4 eV and p_6: 156.0 eV) is identified as well. As reported in the literature [59,60], oxidized Bi species typically exhibits Bi^{3+} state. The spectra in Fig. 4(b) fit well with characteristic peaks of Bi^{3+} along with Bi^{0}, although the curve is not as smooth as that in Fig. 4(a). The primary Bi^{3+} species in reduced 1% Pt–0.5% Bi, suggested by Fig. 4(b), is consistent with our H_2-TPR results (see Table 4 and Fig. 2). Note that partially reduced Bi is likely because of the *ex-situ* XPS measurements since Bi^{0} can be oxidized quickly in air [53].

As shown in Fig. 5, TEM-EDX mapping of 1% Pt–0.5% Bi was performed to further investigate interaction between Pt and Bi on the AC support. As compared with the TEM scan in Fig. 5(a), Fig. 5(b) shows entire background of the AC support, while Fig. 5(c) and (d) demonstrate that all nano-partilces contain both Pt and Bi elements. This suggests that the sequential impregnation approach used in the present study led to bimetallic nano-particles, in which Pt and Bi are closely neighbored with each other, indicating strong interaction.

Table 5
Representative product compositions of methanol low-temperature oxidation under standard operating conditions.

Product, wt%	1% Pt	1% Pt–0.5% Bi	2% Bi
Methanol	89.6	91.9	99.4
Formaldehyde	0.01	7.95	0.06
Methyl formate	2.44	0.03	0.21
Dimethoxymethane	1.08	0.01	0.12
Formic acid	2.39	0.06	0.16
CO_2	4.48	0.05	0.05

3.2. Correlation of catalyst properties with performance

The representative product compositions for low temperature oxidation of methanol under standard operating conditions are shown in Table 5. Over all three catalysts, formaldehyde, methyl formate, dimethoxymethane, formic acid and CO_2 were detected as products. As noted in Introduction, formaldehyde is the target product in the present work. Over 1% Pt, the selectivity toward formaldehyde was low, although methanol conversion (10.4%) was slightly higher than for 1% Pt–0.5% Bi catalyst (8.1%). In

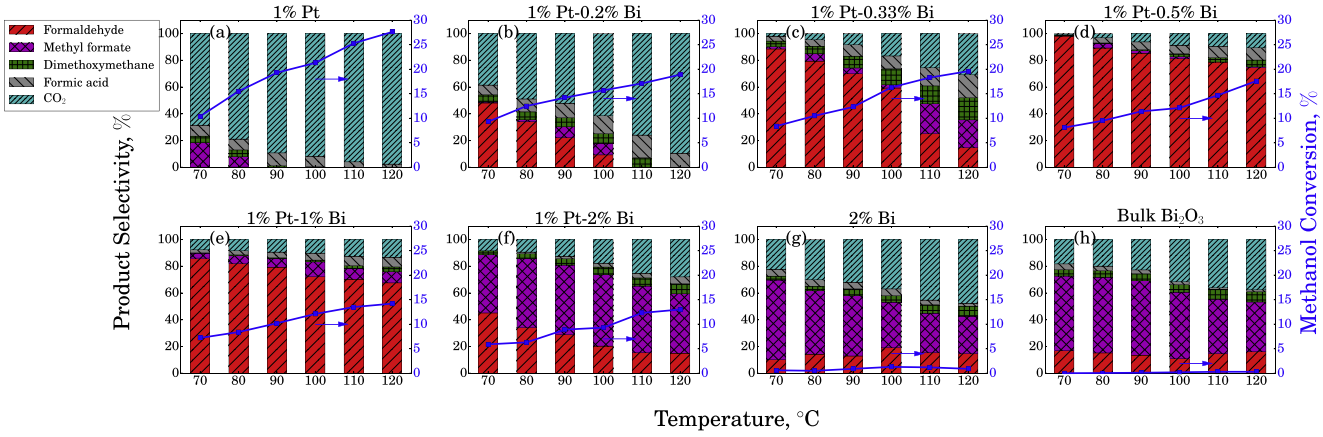


Fig. 6. Methanol conversion and selectivity toward formaldehyde over various catalytic materials, (a)–(f) referring to 1% Pt-*y* % Bi catalysts, when y = (a) 0, (b) 0.2, (c) 0.33, (d) 0.5, (e) 1, (f)2; (g) for 2% Bi and (h) for bulk Bi_2O_3.

contrast, over 2.0% Bi catalyst, methanol conversion was low (0.6%). Preferably, 1% Pt–0.5% Bi gave a high formaldehyde selectivity (98.1%) with methanol conversion 8.1%. Table 5 describes that in the presence of Pt, Bi selectively promotes formaldehyde formation. Similar reactions, converting alcohols to aldehydes using molecular oxygen by selective cleavages of C-H and O-H bonds at the same carbon atom, were reported in our prior works and literature [35,36,40,53,61–64].

Methanol conversion and selectivity toward formaldehyde over various catalytic materials are shown in Fig. 6, where (a), (d) and (g) correspond to the three catalysts used in Table 5. All eight catalysts from Fig. 6 demonstrate clearly that with temperature increase, methanol conversion increases, while selectivity toward formaldehyde decreases. Fig. 6(a) shows that without Bi addition, formaldehyde selectivity is close to zero in the temperature range 70–120 °C, although methanol conversion reaches about 28% at 120 °C. With addition of only 0.2% Bi to 1% Pt (Fig. 6(b)), formaldehyde at 70 °C exhibits ca. 50% selectivity, although it drops to less than 5% at 120 °C. Fig. 6(c), with higher selectivity toward formaldehyde (90–15%), gave similar trend as compared to Fig. 6 (b). For Fig. 6(d) and (e) (Bi contents 0.5% and 1%, respectively), selectivity toward formaldehyde shows relatively high and stable trend with temperature increase. For 2% Bi content (Fig. 6(f)), however, selectivities toward formaldehyde at both 70 and 120 °C are less as compared with 0.5% and 1% Bi contents. In the absence of Pt, illustrated by Fig. 6(g) and (h), methanol conversions are less than 2%, indicating that Pt is necessary to activate methanol and/or O_2. Overall, Fig. 6 shows that at 70 °C (close to methanol boiling point 65 °C), specific Pt-Bi bimetallic catalysts provide high formaldehyde selectivity with methanol conversion ~8%.

Fig. 7 shows that methanol is selectively converted to formaldehyde for 1–8 h TOS, although selectivity towards formaldehyde decreased slightly over this period (from 98.1% to 94.4%). As shown in Table 4, the H_2-TPR measurement was also carried out for used 1% Pt–0.5% Bi. When compared with the fresh 1% Pt–0.5% Bi sample (reducibility 86.3%), reducibility of the used catalyst gave similar but slightly higher value (88.2%). The TPO measurement of used 1% Pt-0.5% Bi catalyst is shown in Fig. 8, where only one sharp peak at 440 °C is found. By integrating the curve in Fig. 8, the amount of accumulated deposited carbon species was obtained. It is remarkable that only small amount of deposit (10.5 mg/g_{cat}) was determined over the used 1% Pt–0.5% Bi catalyst. These observations demonstrate that the 1% Pt–0.5% Bi catalyst exhibits stable performance for methanol selective oxidation to formaldehyde.

In Fig. 9, at 70 °C, the influence of Bi content in Pt-Bi catalysts on methanol conversion, formaldehyde selectivity, Pt dispersion and reducibility is plotted. It shows that with increase of Bi, both Pt dispersion (also see Table 3) and methanol conversion decrease slightly. This leads to essentially the same TOF (turnover frequency, methanol molecules reacted per active Pt site per second, as shown in Table 3) [65]. The Pt dispersion decrease was likely because more Bi segregation occurred over Pt surface when more

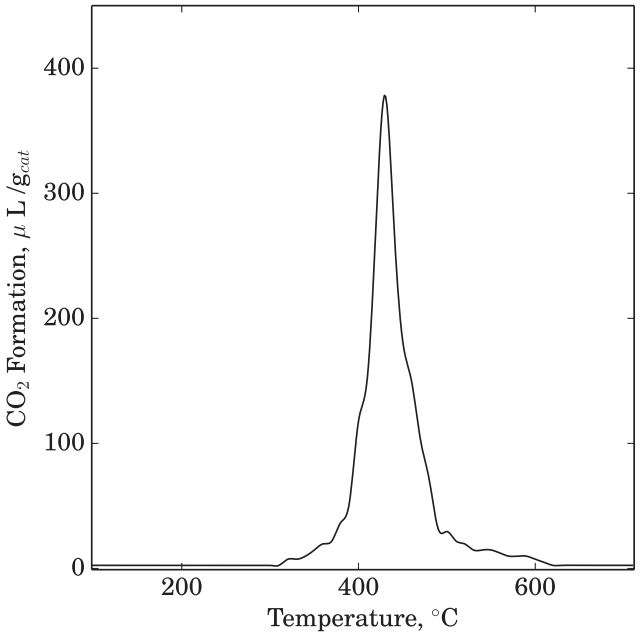


Fig. 8. Temperature-Programmed Oxidation (TPO) profile for used 1% Pt-0.5% Bi catalyst.

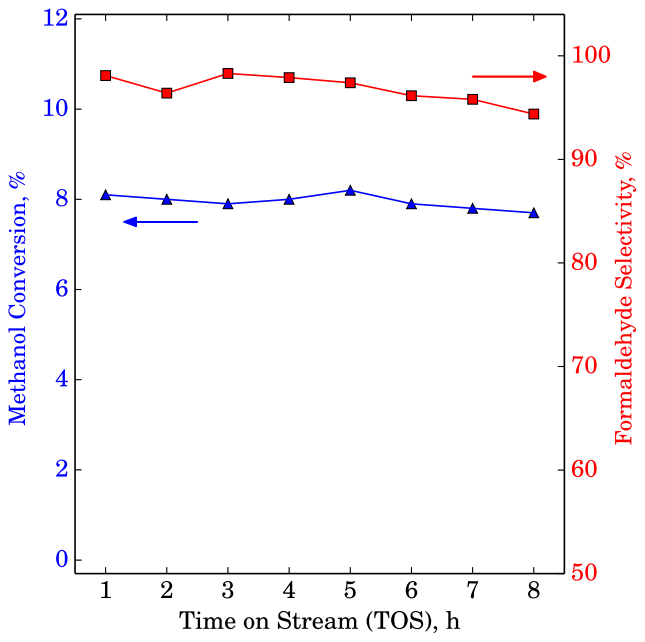


Fig. 7. Catalyst stability for 1% Pt-0.5% Bi under standard operating conditions.

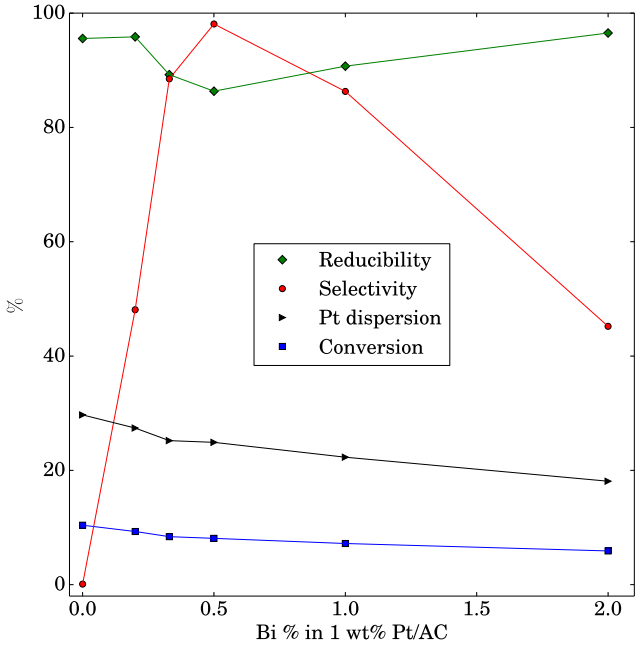


Fig. 9. Influence of Bi content on reducibility, formaldehyde selectivity, Pt dispersion and methanol conversion.

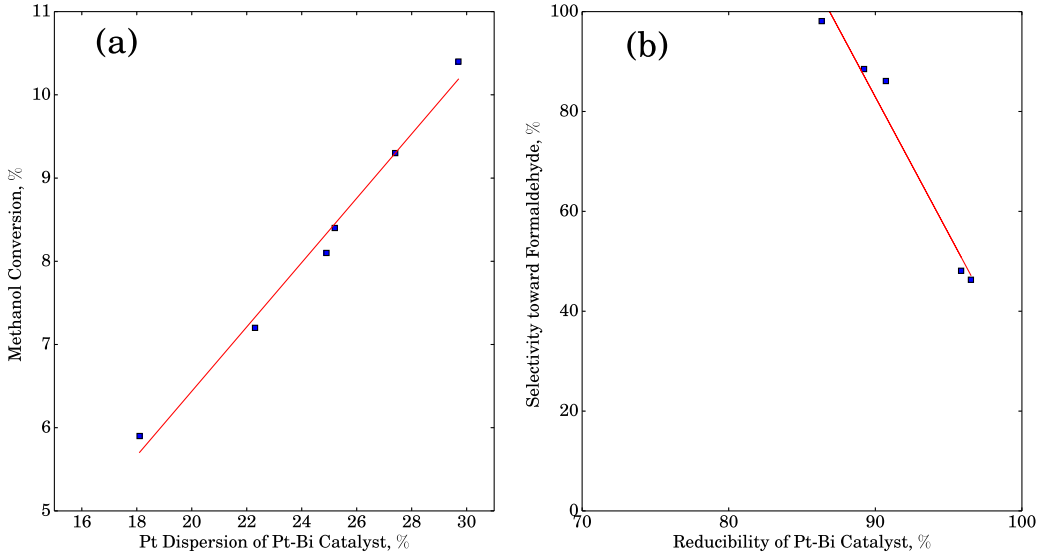


Fig. 10. Correlations of (a) Pt dispersion vs. methanol conversion and (b) reducibility vs. formaldehyde selectivity.

Bi was added to Pt catalysts [40]. The selectivity toward formaldehyde exhibits dramatic change with variation of Bi content, reaching the highest value (98.1%) at Bi content 0.5%. The reducibility, as measured by H_2-TPR and defined in Eq. (2), shows an opposite trend from the selectivity curve. These properties can thus be correlated with catalytic performance, as discussed next.

The correlations of Pt dispersion vs. methanol conversion and reducibility vs. formaldehyde selectivity are plotted in Fig. 10. They demonstrate that Pt dispersion and methanol conversion correlate well by a linear fit. It appears that for the temperature range investigated (70–120 °C), the TOF values for methanol conversion over the various Pt-Bi catalysts were essentially constant (about 1.3–1.4 s^{-1} as shown in Table 3). The relationship of Pt-Bi reducibility and formaldehyde selectivity shows a good linear fit as well, showing that for easier Pt-Bi catalyst reduction (i.e. less H_2 required to fully reduce catalyst), the formaldehyde selectivity is higher. Similar trends for reducibility have also been reported previously for other reactions [66–68].

Fig. 6(a) presents that the monometallic Pt catalyst gives no formaldehyde from methanol oxidation, which is likely because of Pt ensemble effects [69,70]. The addition of a promoter to Pt catalysts leads to both ensemble and electronic effects, causing attenuated chemisorption of small molecules [71,72]. Note that the optimal Pt:Bi weight ratio changes for different reactants, e.g. Pt:Bi = 5:1 for glycerol oxidation [35] and Pt:Bi = 2:1 for methanol oxidation in the present work. As reported in our prior work [40] and literature [73], Bi typically segregates at Pt surfaces in Pt-Bi bimetallic catalysts, functioning as a site blocker [74], and leading to tunable selectivity towards target products [39] and/or better stability [37]. Therefore, relatively more Bi addition is favorable for smaller molecules. Too much Bi addition, however, may result in isolated monometallic Bi particles and weaker interaction between the two metals. This is the likely reason for the optimal reducibility and selectivity of the 1% Pt–0.5% Bi for methanol oxidation to formaldehyde in the present study. As proposed in our prior work [40] and shown in Table 4 and Fig. 2, it appears that in the presence of molecular oxygen, both Pt and Bi are oxidized. With preferable weight ratios of Pt:Bi (1:1–5:1) in the present work, the two metals interact strongly, likely creating Pt^{2+} and partially lower oxidized state than Bi^{3+} as the active site for selective oxidation of methanol. This specific catalyst type appears to favor cleavage of O-H and C-H bonds from the same carbon atom. Following a similar mechanism as proposed in our prior work [40], methanol molecules are adsorbed at Pt surfaces, followed by simultaneous cleavages of O-H and C-H bonds at the oxide interface of Pt and Bi metals, eventually forming water and formaldehyde.

4. Concluding remarks

In the present work, various Pt-Bi bimetallic catalysts were designed, prepared, characterized by BET, ICP-AES, H_2-TPR, TEM, TEM-EDX, TPO, XPS and XRD techniques, and tested in a fixed-bed reactor for low-temperature (70–120 °C) methanol selective oxidation, generating formaldehyde as the target product. The highest selectivity toward formaldehyde was 98% over the 1% Pt–0.5% Bi catalyst at 70 °C, with methanol conversion 8.1%. The catalytic performance correlated well with properties of the Pt-Bi bimetallic catalysts. In particular, the reducibility of Pt-Bi catalysts exhibits a linear relationship with formaldehyde selectivity, while methanol TOF values are essentially constant. As compared to commercial formaldehyde manufacture techniques, this work provides a new catalyst candidate under relatively low temperatures, leading to potentially lower operating costs and capital investment. This work may also offer opportunities for selective oxidation of other alcohols (e.g. ethanol) under low temperatures.

Acknowledgments

This work was supported by the R. Games Slayter and the William and Cynthia Smith gift funds. Y.W. gratefully acknowledges a scholarship from the China Scholarship Council.

References

[1] S.E. Davis, M.S. Ide, R.J. Davis, Selective oxidation of alcohols and aldehydes over supported metal nanoparticles, Green Chem. 15 (2013) 17–45.
[2] T. Mallat, A. Baiker, Oxidation of alcohols with molecular oxygen on solid catalysts, Chem. Rev. 104 (6) (2004) 3037–3058.
[3] F.B. Noronha, E.C. Fendley, R.R. Soares, W.E. Alvarez, D.E. Resasco, Correlation between catalytic activity and support reducibility in the CO_2 reforming of methane over $Pt/Ce_xZr_{1-x}O_2$ catalysts, Chem. Eng. J. 82 (1) (2001) 21–31.
[4] C. Baltes, S. Vukojevic, F. Schuth, Correlations between synthesis, precursor, and catalyst structure and activity of a large set of $CuO/ZnO/Al_2O_3$ catalysts for methanol synthesis, J. Catal. 258 (2) (2008) 334–344.
[5] G. Reuss, W. Disteldorf, A.O. Gamer, A. Hilt, Formaldehyde, in: Ullmann's Encyclopedia of Industrial Chemistry, 2000.
[6] G.J. Millar, M. Collins, Industrial production of formaldehyde using polycrystalline silver catalyst, Ind. Eng. Chem. Res. 56 (33) (2017) 9247–9265.

[7] J. Tatibouet, Methanol oxidation as a catalytic surface probe, Appl. Catal. A: Gen. 148 (2) (1997) 213–252.
[8] M. Badlani, I.E. Wachs, Methanol: a "smart" chemical probe molecule, Catal. Lett. 75 (3) (2001) 137–149.
[9] J.R. Masson, D. McKee, Formaldehyde, in: Van Nostrand's Encyclopedia of Chemistry, 2005.
[10] A.P.V. Soares, M.F. Portela, A. Kiennemann, Methanol selective oxidation to formaldehyde over iron-molybdate catalysts, Catal. Rev. 47 (1) (2005) 125–174.
[11] R.Z. Khaliullin, A.T. Bell, A density functional theory study of the oxidation of methanol to formaldehyde over vanadia supported on silica, titania, and zirconia, J. Phys. Chem. B 106 (32) (2002) 7832–7838.
[12] J. Dobler, M. Pritzsche, J. Sauer, Oxidation of methanol to formaldehyde on supported vanadium oxide catalysts compared to gas phase molecules, J. Am. Chem. Soc. 127 (31) (2005) 10861–10868.
[13] T. Kropp, J. Paier, J. Sauer, Support effect in oxide catalysis: methanol oxidation on vanadia/ceria, J. Am. Chem. Soc. 136 (41) (2014) 14616–14625.
[14] T. Popov, D. Klissurski, K. Ivanov, J. Pesheva, Effect of ultrasonic treatment on the physicochemical properties of Cr-Mo-O catalysts for methanol oxidation, vol. 31, 1987, pp. 191–197.
[15] D. Klissurski, V. Rives, Y. Pesheva, I. Mitov, N. Abadzhjieva, Iron-chromium-molybdenum oxide catalysts for methanol oxidation, Catal. Lett. 18 (3) (1993) 265–271.
[16] D.S. Lafyatis, G. Creten, G.F. Froment, TAP reactor study of the partial oxidation of methanol to formaldehyde using an industrial Fe-Cr-Mo oxide catalyst, Appl. Catal. A: Gen. 120 (1) (1994) 85–103.
[17] Z. Han, W. Pan, W. Pan, J. Li, Q. Zhu, K. Tin, N. Wong, Preparation and effect of Mo-V-Cr-Bi-Si oxide catalysts on controlled oxidation of methane to methanol and formaldehyde, Korean J. Chem. Eng. 15 (5) (1998) 496–499.
[18] A.A. Said, M.M.A. El-Wahab, A.M. Alian, New approach on the catalytic oxidation of methanol to formaldehyde over MoO_3 supported on nano hydroxyapatite catalysts, IOP Conf. Ser.: Mater. Sci. Eng. 64 (1) (2014) 012058.
[19] N. Arora, G. Deo, I.E. Wachs, A.M. Hirt, Surface aspects of bismuth metal oxide catalysts, J. Catal. 159 (1) (1996) 1–13.
[20] V. Diakov, B. Blackwell, A. Varma, Methanol oxidative dehydrogenation in a catalytic packed-bed membrane reactor: experiments and model, Chem. Eng. Sci. 57 (9) (2002) 1563–1569.
[21] V. Diakov, A. Varma, Methanol oxidative dehydrogenation in a packed-bed membrane reactor: yield optimization experiments and model, Chem. Eng. Sci. 58 (3) (2003) 801–807.
[22] L.R. Merte, M. Ahmadi, F. Behafarid, L.K. Ono, E. Lira, J. Matos, L. Li, J.C. Yang, B. Roldan Cuenya, Correlating catalytic methanol oxidation with the structure and oxidation state of size-selected Pt nanoparticles, ACS Catal. 3 (7) (2013) 1460–1468.
[23] W. Diao, J.M.M. Tengco, J.R. Regalbuto, J.R. Monnier, Preparation and characterization of Pt-Ru bimetallic catalysts synthesized by electroless deposition methods, ACS Catal. 5 (9) (2015) 5123–5134.
[24] T.R. Garrick, W. Diao, J.M. Tengco, E.A. Stach, S.D. Senanayake, D.A. Chen, J.R. Monnier, J.W. Weidner, The effect of the surface composition of Ru-Pt bimetallic catalysts for methanol oxidation, Electrochim. Acta 195 (2016) 106–111.
[25] W. Tu, Y.H.C. Chin, Catalytic consequences of chemisorbed oxygen during methanol oxidative dehydrogenation on Pd clusters, ACS Catal. 5 (6) (2015) 3375–3386.
[26] Z. Wu, S. Goel, M. Choi, E. Iglesia, Hydrothermal synthesis of LTA-encapsulated metal clusters and consequences for catalyst stability, reactivity, and selectivity, J. Catal. 311 (2014) 458–468.
[27] A.S. Duke, K. Xie, J.R. Monnier, D.A. Chen, Superior long-term activity for a Pt-Re alloy compared to pt in methanol oxidation reactions, Surf. Sci. 657 (2017) 35–43.
[28] G.L. Chiarello, M.H. Aguirre, E. Selli, Hydrogen production by photocatalytic steam reforming of methanol on noble metal-modified TiO_2, J. Catal. 273 (2) (2010) 182–190.
[29] H. Tatsumi, F. Liu, H.L. Han, L.M. Carl, A. Sapi, G.A. Somorjai, Alcohol oxidation at platinum-gas and platinum-liquid interfaces: the effect of platinum nanoparticle size, water coadsorption, and alcohol concentration, J. Phys. Chem. C 121 (13) (2017) 7365–7371.
[30] A. Wittstock, V. Zielasek, J. Biener, C.M. Friend, M. Baumer, Nanoporous gold catalysts for selective gas-phase oxidative coupling of methanol at low temperature, Science 327 (5963) (2010) 319–322.
[31] G.T. Whiting, S.A. Kondrat, C. Hammond, N. Dimitratos, Q. He, D.J. Morgan, N.F. Dummer, J.K. Bartley, C.J. Kiely, S.H. Taylor, G.J. Hutchings, Methyl formate formation from methanol oxidation using supported gold-palladium nanoparticles, ACS Catal. 5 (2) (2015) 637–644.
[32] R.A. van Santen, I. Tranca, E.J. Hensen, Theory of surface chemistry and reactivity of reducible oxides, Catal. Today 244 (2015) 63–84.
[33] E. Mamedov, Site isolation based design of selective oxidation catalysts, Appl. Catal. A: Gen. 474 (2014) 34–39.
[34] R.A. Puigdollers, P. Schlexer, S. Tosoni, G. Pacchioni, Increasing oxide reducibility: the role of metal/oxide interfaces in the formation of oxygen vacancies, ACS Catal. 7 (10) (2017) 6493–6513.
[35] W. Hu, D. Knight, B. Lowry, A. Varma, Selective oxidation of glycerol to dihydroxyacetone over Pt-Bi/C catalyst: optimization of catalyst and reaction conditions, Ind. Eng. Chem. Res. 49 (21) (2010) 10876–10882.
[36] W. Hu, B. Lowry, A. Varma, Kinetic study of glycerol oxidation network over Pt-Bi/C catalyst, Appl. Catal. B: Environ. 106 (1–2) (2011) 123–132.
[37] Y. Xiao, A. Varma, Catalytic deoxygenation of guaiacol using methane, ACS Sust. Chem. Eng. 3 (11) (2015) 2606–2610.
[38] Y. Xiao, A. Varma, Kinetics of guaiacol deoxygenation using methane over the Pt-Bi catalyst, React. Chem. Eng. 2 (1) (2017) 36–43.
[39] Y. Xiao, A. Varma, Highly selective nonoxidative coupling of methane over Pt-Bi bimetallic catalysts, ACS Catal. 8 (4) (2018) 2735–2740.
[40] Y. Xiao, J. Greeley, A. Varma, Z.J. Zhao, G. Xiao, An experimental and theoretical study of glycerol oxidation to 1,3-dihydroxyacetone over bimetallic Pt-Bi catalysts, AIChE J. 63 (2) (2017) 705–715.
[41] J.E. Benson, M. Boudart, Hydrogen-oxygen titration method for the measurement of supported platinum surface areas, J. Catal. 4 (6) (1965) 704–710.
[42] M.T. Paffett, C.T. Campbell, R.G. Windham, B.E. Koel, A multitechnique surface analysis study of the adsorption of H_2, CO and O_2 on BiPt(111) surfaces, Surf. Sci. 207 (2) (1989) 274–296.
[43] Z. Shang, M. Sun, S. Chang, X. Che, X. Cao, L. Wang, Y. Guo, W. Zhan, Y. Guo, G. Lu, Activity and stability of CO_3O_4-based catalysts for soot oxidation: the enhanced effect of Bi_2O_3 on activation and transfer of oxygen, Appl. Catal. B: Environ. 209 (2017) 33–44.
[44] C.P. Hwang, C.T. Yeh, Platinum-oxide species formed by oxidation of platinum crystallites supported on alumina, J. Mol. Catal. A: Chem. 112 (2) (1996) 295–302.
[45] L. Zhou, W. Wang, H. Xu, S. Sun, M. Shang, Bi_2O_3 hierarchical nanostructures: controllable synthesis, growth mechanism, and their application in photocatalysis, Chem. – A Eur. J. 15 (7) (2009) 1776–1782.
[46] G. Sethia, A. Sayari, Activated carbon with optimum pore size distribution for hydrogen storage, Carbon 99 (2016) 289–294.
[47] E. Antolini, J.R. Salgado, E.R. Gonzalez, The stability of Pt-M (M = first row transition metal) alloy catalysts and its effect on the activity in low temperature fuel cells: a literature review and tests on a Pt-Co catalyst, J. Power Sources 160 (2) (2006) 957–968.
[48] C. Fischer, R. Thede, W. Baumann, H.J. Drexler, A. Konig, D. Heller, Investigations into metal leaching from polystyrene-supported rhodium catalysts, ChemCatChem 8 (2) (2016) 352–356.
[49] Z. Wu, E.C. Wegener, H.T. Tseng, J.R. Gallagher, J.W. Harris, R.E. Diaz, Y. Ren, F. H. Ribeiro, J.T. Miller, Pd-In intermetallic alloy nanoparticles: highly selective ethane dehydrogenation catalysts, Catal. Sci. Technol. 6 (2016) 6965–6976.
[50] Y. Xiao, A. Varma, Conversion of glycerol to hydrocarbon fuels via bifunctional catalysts, ACS Energy Lett. 1 (5) (2016) 963–968.
[51] Z. Zhu, G. Lu, Y. Guo, Y. Guo, Z. Zhang, Y. Wang, X.Q. Gong, High performance and stability of the Pt-W/ZSM-5 catalyst for the total oxidation of propane: the role of tungsten, ChemCatChem 5 (8) (2013) 2495–2503.
[52] G. Ertl, H. Knozinger, F. Schuth, J. Weitkamp, Handbook of Heterogeneous Catalysis: 312 Particle Size and Dispersion Measurements, second ed., vol. 1, Wiley–VCH, Weinheim, Germany, 2008, pp. 738 – 765.
[53] T. Lu, Z. Du, J. Liu, H. Ma, J. Xu, Aerobic oxidation of primary aliphatic alcohols over bismuth oxide supported platinum catalysts in water, Green Chem. 15 (2013) 2215–2221.
[54] W.W. Liu, Y.S. Feng, G.Y. Wang, W.W. Jiang, H.J. Xu, Characterization and reactivity of γ-Al_2O_3 supported Pd-Cu bimetallic nanocatalysts for the selective oxygenization of cyclopentene, Chin. Chem. Lett. 27 (6) (2016) 905–909.
[55] J.A.H. Dreyer, S. Pokhrel, J. Birkenstock, M.G. Hevia, M. Schowalter, A. Rosenauer, A. Urakawa, W.Y. Teoh, L. Madler, Decrease of the required dopant concentration for [small Delta]-Bi_2O_3 crystal stabilization through thermal quenching during single-step flame spray pyrolysis, CrystEngComm 18 (2016) 2046–2056.
[56] N. Wagstaff, R. Prins, Alloy formation and metal oxide segregation in PtRe/γ-Al_2O_3 catalysts as investigated by temperature-programmed reduction, J. Catal. 59 (3) (1979) 434–445.
[57] P. Bera, K.R. Priolkar, A. Gayen, P.R. Sarode, M.S. Hegde, S. Emura, R. Kumashiro, V. Jayaram, G.N. Subbanna, Ionic dispersion of Pt over CeO_2 by the combustion method: structural investigation by XRD, TEM, XPS, and EXAFS, Chem. Mater. 15 (10) (2003) 2049–2060.
[58] K. Asami, T. Osaka, T. Yamanobe, I. Koiwa, Metallic bismuth on strontium-bismuth tantalate thin films for ferroelectric memory application, Surf. Interf. Anal. 30 (1) (2000) 391–395.
[59] L. Zhang, P. Ghimire, J. Phuriragpitikhon, B. Jiang, A.A. Goncalves, M. Jaroniec, Facile formation of metallic bismuth/bismuth oxide heterojunction on porous carbon with enhanced photocatalytic activity, J. Colloid Interf. Sci. 513 (2018) 82–91.
[60] M. Wenkin, C. Renard, P. Ruiz, B. Delmon, M. Devillers, On the role of bismuth-based alloys in carbon-supported bimetallic Bi-Pd catalysts for the selective oxidation of gluconic acid, in: Heterogeneous Catalysis and Fine Chemicals IV: Proceedings of the 4th International Symposium on Heterogeneous Catalysis and Fine Chemicals, vol. 108, 1997, pp. 391–398.
[61] T. Mallat, Z. Bodnar, P. Hug, A. Baiker, Selective oxidation of cinnamyl alcohol to cinnamaldehyde with air over Bi-Pt/alumina catalysts, J. Catal. 153 (1) (1995) 131–143.
[62] J. Xie, B. Huang, K. Yin, H.N. Pham, R.R. Unocic, A.K. Datye, R.J. Davis, Influence of dioxygen on the promotional effect of Bi during Pt-catalyzed oxidation of 1,6-hexanediol, ACS Catal. 6 (7) (2016) 4206–4217.
[63] J. Liu, S. Zou, H. Wang, L. Xiao, H. Zhao, J. Fan, Synergistic effect between Pt^0 and Bi_2O_{3-x} for efficient room-temperature alcohol oxidation under base-free aqueous conditions, Catal. Sci. Technol. 7 (2017) 1203–1210.
[64] K. Yang, J. Li, Y. Peng, J. Lin, Enhanced visible light photocatalysis over Pt-loaded Bi_2O_3: an insight into its photogenerated charge separation, transfer and capture, Chem. Commun. 19 (2017) 251–257.

[65] M. Boudart, Turnover rates in heterogeneous catalysis, Chem. Rev. 95 (3) (1995) 661–666.
[66] V.d.O. Rodrigues, J.G. Eon, A.C. Faro, Correlations between dispersion, acidity, reducibility, and propane aromatization activity of gallium species supported on HZSM5 zeolites, J. Phys. Chem. C 114 (10) (2010) 4557–4567.
[67] J.L. Ayastuy, A. Gurbani, M. Gonzalez-Marcos, M. Gutierrez-Ortiz, Selective CO oxidation in H_2 streams on CuO/$Ce_xZr_{1-x}O_2$ catalysts: correlation between activity and low temperature reducibility, Int. J. Hydrogen Energy 37 (2) (2012) 1993–2006.
[68] G. Kumar, S.L.J. Lau, M.D. Krcha, M.J. Janik, Correlation of methane activation and oxide catalyst reducibility and its implications for oxidative coupling, ACS Catal. 6 (3) (2016) 1812–1821.
[69] M.S. Kumar, D. Chen, A. Holmen, J.C. Walmsley, Dehydrogenation of propane over Pt-SBA-15 and Pt-Sn-SBA-15: effect of Sn on the dispersion of Pt and catalytic behavior, Catal. Today 142 (1) (2009) 17–23.
[70] T. Duan, R. Zhang, L. Ling, B. Wang, Insights into the effect of Pt atomic ensemble on HCOOH oxidation over Pt-decorated Au bimetallic catalyst to maximize Pt utilization, J. Phys. Chem. C 120 (4) (2016) 2234–2246.
[71] M.T. Paffett, C.T. Campbell, T.N. Taylor, The influence of adsorbed Bi on the chemisorption properties of Pt(111): H_2, CO, and O_2, J. Vac. Sci. Technol. A: Vacuum Surf. Films 3 (3) (1985) 812–816.
[72] R.G. Windham, B.E. Koel, M.T. Paffett, Studies of the ensemble size requirements for ethylene adsorption and decomposition on platinum(111): ethylene and bismuth coadsorption, Langmuir 4 (5) (1988) 1113–1118.
[73] J. Campbell, C.T. Campbell, The interactions of cyclopentane with clean and bismuth-covered Pt(111), Surface Sci. 210 (1) (1989) 46–68.
[74] H. Kimura, K. Tsuto, T. Wakisaka, Y. Kazumi, Y. Inaya, Selective oxidation of glycerol on a platinum-bismuth catalyst, Appl. Catal. A: Gen. 96 (2) (1993) 217–228.